Jpn. J. Appl. Phys. Vol. 38 (1999) pp. L 1243–L 1245
Part 2, No. 11A, 1 November 1999

Spectral Phase-Locking in Ultrafast All-Optical Mach-Zehnder-Type Semiconductor Wavelength Converters

Yoshiyasu UENO*, Shigeru NAKAMURA and Kazuhito TAJIMA
Optoelectronics and High-Frequency Device Research Laboratories, NEC Corporation, 34 Miyukigaoka, Tsukuba, Ibaraki 305-8501, Japan

(Received August 2, 1999; accepted for publication September 8, 1999)

We studied the spectrum-domain mechanism of the delayed-interference signal-wavelength converter (DISC) analytically and found that the role of the passive Mach-Zehnder interferometer in this converter differs completely from that of conventional spectrum filters: it converts the semiconductor-optical-amplifier-induced cross-phase-modulated spectrum phase from out-of-phase to in-phase (constant phase). This converter therefore efficiently generates ultrashort nearly transform-limited pulses having a broad phase-locked spectrum. These conclusions are consistent with the output pulse shapes and spectra measured in experiments in which the wavelength of 2-ps 42-GHz pulses was converted from 1560 nm to 1553 nm.

KEYWORDS: wavelength conversion, all-optical, semiconductor, Mach-Zehnder interferometer, transform-limited, spectrum filter

All-optical wavelength converters[1] will significantly enhance the cross-connecting flexibility of wavelength-division-multiplexed (WDM) communication systems. The response time of these converters, though, is important for increasing the system capacity because increasing the number of WDM channels inevitably reduces the signal quality as a result of the cross-phase modulation during transmission. We previously proposed an ultrafast wavelength converter that we call a delayed-interference signal-wavelength converter (DISC).[2–4] It is a simple structure consisting of a semiconductor optical amplifier (SOA) followed by a passive asymmetric Mach-Zehnder (MZ) interferometer. Its response time is not limited by the semiconductor carrier's lifetime as we have demonstrated by showing that it can generate 7-ps 42-GHz 1560-nm wavelength-converted pulses from extremely low-power (6 fJ/pulse) 5-ps 42-GHz 1548-nm input pulses. The time-domain mechanism of the DISC is in principle exactly the same as that of the so-called symmetric-Mach-Zehnder switch structure,[5–7] which has been intensively studied and used for various all-optical functions[8–11] because of its ultrafast response. The DISC mechanism in the spectrum domain, in contrast, has not been studied. The passive MZ interferometer after the SOA, for example, appears to work as a spectrum filter, but the role of this filter in the wavelength conversion has not been identified. The chirp property of the converted output pulses, which is important for transmitting these pulses, has not been studied, either.

In the work reported here we studied the spectrum-domain mechanism of all-optical semiconductor wavelength converters analytically and found that the role of the MZ interferometer differs completely from those of conventional filters used in other all-optical wavelength converters and switches that consist of nonlinear waveguides followed by filters (an optical fiber and a filter,[12] or a semiconductor waveguide and a filter[13,14]).

The DISC consists of a polarization-insensitive bulk-InGaAsP SOA and a MZ interferometer (Fig. 1). Input pulses (λ_1) and co-propagating continuous-wave (CW) input light (λ_2) enter the DISC. The input pulse width is much shorter than the carrier lifetime, the MZ delay time (between its two arms) is set close to the input pulse width, and the MZ phase difference is adjusted so that the CW wavelength components

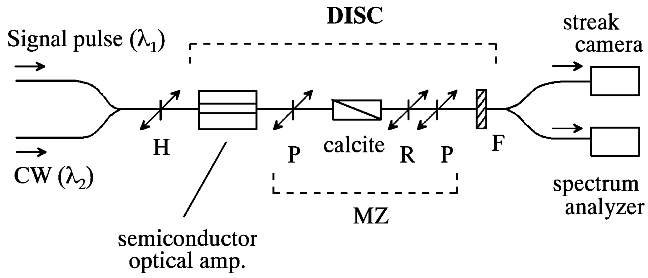

Fig. 1. Experimental setup of the delayed-interference signal-wavelength converter (DISC). H: half-wave plate, R: phase retarder, P: polarizer, F: bandpass filter.

(λ_2) interfere destructively. The width of the output pulse is determined by the MZ's delay time.[2,3] As a consequence, the DISC converts the pulse wavelength from λ_1 to λ_2, without being limited by the carrier lifetime.

The λ_2 CW light is cross-phase modulated (XPM) inside the SOA by the λ_1 input pulses and the destructive interference in the MZ interferometer filters out the remaining λ_2 CW component. Our experimental setup (Fig. 1) used the interference between orthogonally-polarized λ_2 beams co-propagating through a birefringent calcite crystal instead of the interference between two spatially split beams. The MZ delay time was determined by the length of the calcite crystal, and the MZ phase difference was tuned by an optical-phase retarder (a Babinet-Soleil compensator). A conventional bandpass filter placed after the SOA removed the amplified λ_1 input pulses and most of the amplified spontaneous emission from the SOA, but passed all the XPM components with wavelengths near λ_2.

Our attention in this work was on the phase spectrum of the XPM components throughout the DISC's wavelength-conversion process, but the XPM phase spectrum is difficult to measure experimentally. We therefore simulated the DISC operation numerically, assuming the SOA to be driven by 2-ps 42-GHz 11-fJ input pulses. We took into account the nonlinear refractive-index change which is proportional to the carrier-density change (the bandfilling effect), the linear gain, the pulse gain saturation, and the carrier recovery between pulses,[4] but we ignored the so-called ultrafast carrier dynamics because they do not affect the refractive-index change much when the SOA is driven by 2-ps pulses.[15] In these calculations we used SOA parameters measured previ-

*E-mail address: ueno@obl.cl.nec.co.jp

ously: gains of 700 at λ_1 and λ_2, a carrier lifetime (τ_c) of 60 ps, and a pulse saturation energy of 180 fJ.[4]

Figure 2 shows the results calculated for the CW light (λ_2) at the SOA output. Fig. 2(a) shows the intensity modulation due to the SOA-gain modulation, and Fig. 2(b) shows that the CW spectrum is broadened because of the SOA-induced XPM (the spectrum spacing $= 42$ GHz $= 0.34$ nm). Our calculation revealed that the XPM spectrum components above and below the CW wavelength are out of phase with each other (Fig. 2(d)), while the blue and red components are each in-phase (constant phase). The phase difference between the blue and red components is π. We think these are significant properties of semiconductor (SOA) -induced XPM. Our calculations also revealed that the XPM spectrum has these properties in general when the input-pulse repetition rate is higher than the carrier's cutoff frequency ($1/\tau_c$). In such a case, the phase of the CW light as a function of time as well as its intensity have the saw-tooth-like shapes shown in Figs. 2(a) and 2(c). This is because the carrier density recovers linearly in time after each rapid depletion due to the amplification of a short input pulse. We concluded that the out-of-phase XPM spectrum originates from the saw-tooth-shaped phase and intensity modulation. Thus, the SOA-induced XPM differs from the fiber's pure-$\chi^{(3)}$-induced XPM previously used in all-optical switches.[12] The fiber-induced XPM spectrum does not show such a discontinuity in phase.

Figure 3 shows the results calculated for the XPM components at the MZ interferometer output (and also at the DISC output) when the MZ delay time (Δt) was assumed to be 2 ps. Figure 3(a) shows that, as has been explained by the time-domain model, these XPM components form 2-ps 42-GHz pulses. And as shown in Fig. 3(b), because of the destructive interference these is no CW component in the center of the XPM spectrum. Our calculations revealed that this spectrum, unlike the XPM spectrum at the SOA output, is in-phase as shown in Fig. 3(c). It is thus indicated that the phase spectrum of the DISC output pulses is in-phase (constant).

It is also indicated that the MZ interferometer is different from conventional spectrum filters: the MZ interferometer not only filters out the CW component but also converts the XPM spectrum phase from out-of-phase to in-phase. The interferometer's output amplitude in the time domain, $E_{\mathrm{out}}(t)$, is written as

$$E_{\mathrm{out}}(t) = \frac{1}{\sqrt{2}}\left[E_{\mathrm{in}}(t) - E_{\mathrm{in}}(t-\Delta t)\right]. \qquad (1)$$

After we Fourier-transformed this equation, we obtained the spectrum-domain transfer function of the MZ interferometer:

$$S^{\mathrm{MZ}}(\omega) = -\sin[(\omega-\omega_2)\times\Delta t]. \qquad (2)$$

Equation (2) clearly indicates that the MZ interferometer changes the signs of the amplitudes of the spectra of the blue components ($\omega > \omega_2$). Thus, the phase spectra of the blue components shift by π with respect to those of the red components.

Conventional filters cannot play the role played by the MZ interferometer. Multi-layered filters (including fiber Bragg gratings), for example, work as notch filters because of Bragg reflection. If the MZ interferometer in the DISC were replaced with an appropriate notch filter, the filter would remove the CW component and pass the other blue and red components but it would not convert the phase of the XPM spectrum. As shown by the calculation results in Fig. 4, doublet pulses would be generated at the filter output because the blue components would destructively interfere with the out-of-phase red components. If short pulses are to be generated when using such a conventional filter in place of the MZ interferometer, the filter must allow only the blue or only the red components to pass through.[13,14]

We tested these conclusions experimentally and found that the output-pulse shape and spectrum observed at the DISC output, respectively Figs. 5(a) and 5(b), were similar to the calculation results shown in Figs. 3(a) and 3(b). We fed into the SOA 2.0-ps 42-GHz 11-fJ 1560-nm input pulses together with co-propagating 10-μW 1553.1-nm CW light. The MZ delay time was 2.0 ps. Although the pulse width shown in Fig. 5(a) is broadened due to the limited resolution of the streak camera we used, the pulse width determined using an

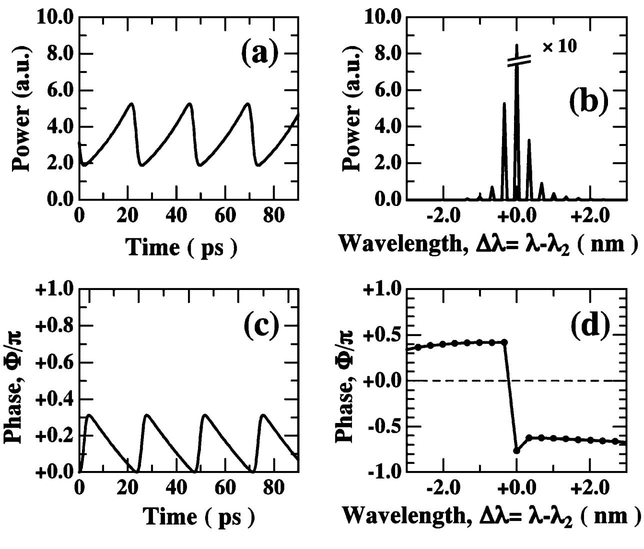

Fig. 2. Calculated properties of the λ_2 light at the SOA output. (a) output power, (b) power spectrum, (c) output amplitude phase, (d) phase spectrum.

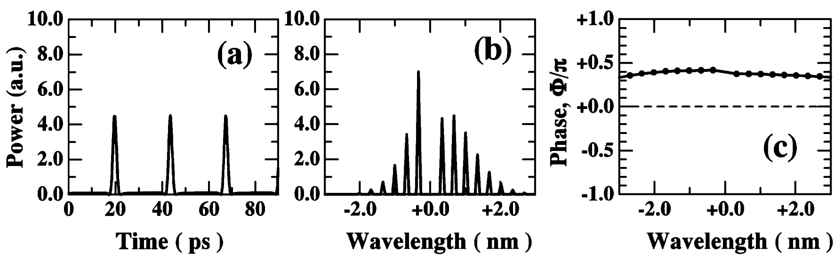

Fig. 3. Calculated properties of the λ_2 light at the DISC output. (a) output power, (b) spectrum, (c) phase spectrum.

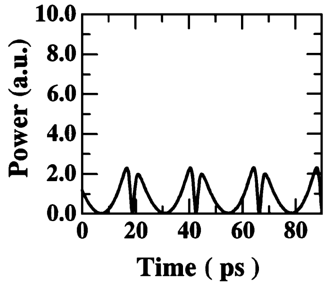

Fig. 4. Calculated properties of the λ_2 light power when a conventional notch filter was assumed to be substituted for the MZ interferometer.

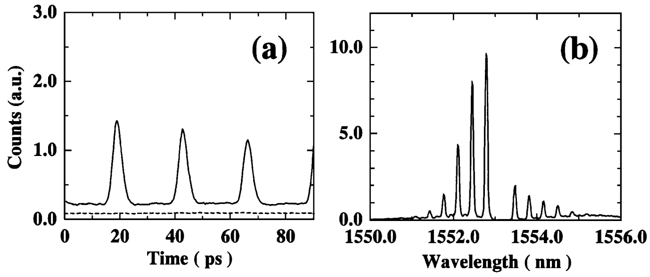

Fig. 5. Measured DISC output. (a) output power (the pulse width was independently determined to be 2 ps), (b) output spectrum.

auto-correlator was approximately 2 ps. (The non uniformity of the pulse height in Fig. 5(a) was simply caused by the non uniformity of the 42-GHz input pulses, which were generated by spatially multiplexing 10.5-GHz mode-locked laser pulses.) The dashed line in Fig. 5(a) shows the background noise level due to amplified spontaneous emission from an Er-doped fiber amplifier placed in front of the streak camera.

The extinction ratio indicated by the output pulses in Fig. 5(a) is poor: the floor level between pulses is above the background noise level (the relative intensity between pulses is exaggerated in Fig. 5(a), because the peak height shown there is antifactually reduced by a factor of 3 because of the limited reslution of the streak camera). The extinction ratio is poor when the output pulse width (the MZ delay time) is not negligibly short with respect to the repetition time but can be improved by optimizing the MZ phase bias.[4)]

The pulse shape and spectrum of the DISC output measured after optimizing the MZ phase bias to 1.04π from π in Fig. 5 are shown in Fig. 6. The phase bias was adjusted using a calibrated phase retarder. After the optimization, the extinction ratio is high and the spectrum envelope is smooth. The time-bandwidth product $[\Delta t \times \Delta f]$ was 0.41. The results of calculations assuming that the phase bias is 1.04π matched these experimental results very well. These calculation results revealed that the output phase spectrum remains almost constant after the optimization.

In conclusion, we have analyzed the spectrum-domain mechanism of an ultrafast all-optical semiconductor wavelength converter and found that the MZ interferometer's role in this converter is fundamentally different from that of spectrum filters: the interferometer converts the XPM spectrum of the SOA output from out-of-phase to in-phase. The DISC therefore generates nearly transform-limited ultrashort pulses. The conclusions drawn from this analysis are consistent with measured results demonstrating the wavelength conversion of 2-ps 42-GHz pulses.

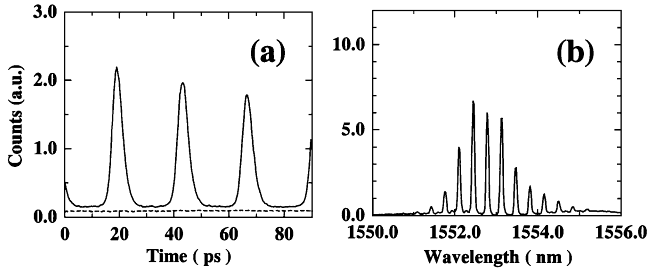

Fig. 6. DISC output measured after optimizing the MZ phase bias. (a) output power, (b) output spectrum.

One of the authors (Y. U.) thanks Dr. Pak S. Cho, Univ. of Maryland for valuable discussions. Part of this work was performed under the management of the Femtosecond Technology Research Association supported by the New Energy and Industrial Technology Development Organization.

1) T. Durhuus, B. Mikkelsen, C. Joergensen, S. L. Danielsen and K. E. Stubkjaer: J. Lightwave Technol. **14** (1996) 942.
2) Y. Ueno, S. Nakamura, K. Tajima and S. Kitamura: IEEE Photonics Technol. Lett. **10** (1998) 346.
3) Y. Ueno, S. Nakamura, K. Tajima and S. Kitamura: *Tech. Dig. 24th European Conf. Optical Communication (ECOC '98), Madrid 1998*, pp. 657–658.
4) Y. Ueno, S. Nakamura and K. Tajima: Opt. Lett. **23** (1998) 1846.
5) K. Tajima: Jpn. J. Appl. Phys. **32** (1993) L1746.
6) K. Tajima, S. Nakamura and Y. Sugimoto: Appl. Phys. Lett. **67** (1995) 3709.
7) S. Nakamura, Y. Ueno and K. Tajima: IEEE Photonics Technol. Lett. **10** (1998) 1575.
8) B. Mikkelsen, K. S. Jepsen, M. Vaa, H. N. Poulsen, K. E. Stubkjaer, R. Hess, M. Duelk, W. Vogt, E. Gamper, E. Gini, P. A. Besse, H. Melchior, S. Bouchoule and F. Devaux: Electron. Lett. **33** (1997) 2137.
9) R. Hess, M. Caraccia-Gross, W. Vogt, E. Gamper, P. A. Besse, M. Duelk, E. Gini, H. Melchior, B. Mikkelsen, M. Vaa, K. S. Jepsen, K. E. Stubkjaer and S. Bouchoule: IEEE Photonics Technol. Lett. **10** (1998) 165.
10) K. L. Hall and K. A. Rauschenbach: Opt. Lett. **23** (1998) 1271.
11) L. Billes, J. C. Simon, B. Kowalski, M. Henry, G. Michaud, P. Lamouler and F. Alard: *Tech. Dig. 23rd European Conf. Optical Communication (ECOC '97), Edinburgh 1997*, Vol. 2, pp. 269–272.
12) T. Morioka, K. Mori and M. Saruwatari: Electron. Lett. **28** (1992) 1070.
13) S. Nakamura and K. Tajima: Appl. Phys. Lett. **70** (1997) 3498.
14) P. S. Cho, D. Margerefteh, J. Goldhar and G. L. Burdge: IEEE Photonics Technol. Lett. **30** (1998) 66.
15) Y. Ueno, S. Nakamura, K. Tajima and S. Ishikawa: *Tech. Dig. 4th Int. Workshop on Femtosecond Technology (FST '97), Tsukuba 1997*, p. 108.